AMERICAN SOCIETY FOR MICROBIOLOGY | Molecular and Cellular Biology

Histone Chaperone Nap1 Is a Major Regulator of Histone H2A-H2B Dynamics at the Inducible *GAL* Locus

Xu Chen,[a]* Sheena D'Arcy,[a,b]* Catherine A. Radebaugh,[a] Daniel D. Krzizike,[a,b] Holli A. Giebler,[a] Liangquan Huang,[a] Jennifer K. Nyborg,[a] Karolin Luger,[a,b,c]* Laurie A. Stargell[a,c]

Department of Biochemistry and Molecular Biology, Colorado State University, Fort Collins, Colorado, USA[a]; Howard Hughes Medical Institute, Colorado State University, Fort Collins, Colorado, USA[b]; Institute for Genome Architecture and Function, Colorado State University, Fort Collins, Colorado, USA[c]

Histone chaperones, like nucleosome assembly protein 1 (Nap1), play a critical role in the maintenance of chromatin architecture. Here, we use the *GAL* locus in *Saccharomyces cerevisiae* to investigate the influence of Nap1 on chromatin structure and histone dynamics during distinct transcriptional states. When the *GAL* locus is not expressed, cells lacking Nap1 show an accumulation of histone H2A-H2B but not histone H3-H4 at this locus. Excess H2A-H2B interacts with the linker DNA between nucleosomes, and the interaction is independent of the inherent DNA-binding affinity of H2A-H2B for these particular sequences as measured *in vitro*. When the *GAL* locus is transcribed, excess H2A-H2B is reversed, and levels of all chromatin-bound histones are depleted in cells lacking Nap1. We developed an *in vivo* system to measure histone exchange at the *GAL* locus and observed considerable variability in the rate of exchange across the locus in wild-type cells. We recapitulate this variability with *in vitro* nucleosome reconstitutions, which suggests a contribution of DNA sequence to histone dynamics. We also find that Nap1 is required for transcription-dependent H2A-H2B exchange. Altogether, these results indicate that Nap1 is essential for maintaining proper chromatin composition and modulating the exchange of H2A-H2B *in vivo*.

The basic unit of chromatin is the nucleosome, which forms when DNA is wrapped around two copies each of the four core histones arranged as two histone H2A-H2B dimers and a histone H3-H4 tetramer (1). Nucleosomes are highly dynamic, capable of multiple structural transitions between completely assembled and entirely disassembled structures (2). Indeed, H2A-H2B and H3-H4 are actively exchanged during both DNA replication-dependent and -independent events (3–9). Chromatin transitions have the potential to profoundly affect gene expression, and a diverse spectrum of factors, including histone chaperones, participate in this process (10).

Histone chaperones are histone-binding proteins that facilitate nucleosome assembly and/or disassembly in an ATP-independent fashion (11–13). The histone chaperone nucleosome assembly protein 1 (Nap1) is a highly conserved chaperone that binds H2A-H2B *in vitro* with nanomolar affinity (12, 14) in a conformation that shields interfaces required for nucleosome assembly (15). Although functional in the assembly of nucleosomes *in vitro* (16), a number of studies support a role for Nap1 in transcription-dependent processes of disassembly of nucleosomes. Nap1 is critical for the eviction of histones during transcription in a mammalian *in vitro* system (17), and Nap1 (with the ATP-dependent chromatin remodeler RSC [remodels the structure of chromatin]) can facilitate the elongation of RNA polymerase II (RNAPII) on chromatin templates using yeast *in vitro* systems (18, 19). Our previous *in vivo* studies indicated that Nap1 prevents excess H2A-H2B accumulation on chromatin (20), and here, we expand our analysis to investigate the role of Nap1 in histone exchange and occupancy. As a model system, we use the *GAL* locus in yeast under transcriptionally repressed and activated conditions.

The *Saccharomyces cerevisiae GAL* gene cluster (*GAL7*, *GAL1*, and *GAL10*) is a powerful system for studying chromatin dynamics *in vivo* under variable levels of gene expression. Transcription of *GAL* genes is repressed in the presence of glucose and coordinately activated in the presence of galactose (21, 22). The region is characterized by high levels of nucleosome occupancy in the repressed state (23–25). Upon activation, histones are acetylated (26–33), and a majority are evicted (24, 34–36) with the help of chromatin-remodeling factors (37) and histone chaperones (38).

Although chromatin structure and histone modifications at the *GAL* locus are well characterized, probing of histone dynamics has been confounded by the fact that typical exchange studies utilize a tagged histone expression system regulated by a galactose-inducible promoter (4–9). We therefore constructed a novel exchange system in which the expression of a hemagglutinin (HA)-tagged histone (^{HA}H2B or H3^{HA}) is regulated by the antibiotic doxycycline. This allowed us to examine histone exchange at these model genes without altering the carbon source. We found that certain nucleosomes are highly dynamic and require Nap1 for high levels of histone H2A-H2B exchange. Nap1 is also needed for maintaining normal histone density and preventing excess H2A-H2B accumulation.

Received 28 August 2015 **Returned for modification** 22 September 2015
Accepted 25 January 2016

Accepted manuscript posted online 16 February 2016

Citation Chen X, D'Arcy S, Radebaugh CA, Krzizike DD, Giebler HA, Huang L, Nyborg JK, Luger K, Stargell LA. 2016. Histone chaperone Nap1 is a major regulator of histone H2A-H2B dynamics at the inducible *GAL* locus. Mol Cell Biol 36:1287–1296. doi:10.1128/MCB.00835-15.

Address correspondence to Laurie A. Stargell, Laurie.Stargell@colostate.edu.

* Present address: Xu Chen, Department of Microbiology, Immunology and Pathology, Colorado State University, Fort Collins, Colorado, USA; Sheena D'Arcy, Department of Chemistry and Biochemistry, University of Texas at Dallas, Dallas, Texas, USA; Karolin Luger, Department of Chemistry and Biochemistry, University of Colorado at Boulder, Boulder, Colorado, USA.

Supplemental material for this article may be found at http://dx.doi.org/10.1128/MCB.00835-15.

MATERIALS AND METHODS

Yeast strains, plasmids, and culture conditions. The following *S. cerevisiae* yeast strains were purchased from Thermo Scientific Open Biosystems: the wild-type (wt) strain (BY4741 *MAT***a** *his3*Δ*1 ura3*Δ*0 leu2*Δ*0 met15*Δ*0*) (catalog number YSC1048) and the *nap1*Δ strain (BY4741 *nap1*Δ::Kan^r) (catalog number YSC6273-201936599). The strain containing tandem affinity purification (TAP)-tagged Htz1 was purchased from GE Dharmacon (BY4741 *Htz1*-TAP::*HIS3MX6*) (catalog number YSC1178-202233238). TAP-tagged *Htz1* in the *nap1*Δ strain was generated by homologous recombination of a PCR product derived from TAP-tagged *Htz1* in the wild-type strain. For replication-independent histone exchange studies, α-factor (catalog number RP01002; GenScript) was added to arrest cells in the G_1 stage. To prevent α-factor degradation by Bar1 (39), a *BAR1* gene deletion strain (*bar1*Δ) (catalog number YSC6273-201920294; Thermo Scientific) was used as the wild type, and the *nap1*Δ strain was generated in this background by using established protocols (40).

Plasmids for doxycycline-regulated ^{HA}H2B and H3^{HA} expression were generated by subcloning from the galactose-regulated plasmids pGAL1 HA-H2B and pGAL1 H3-HA (both containing 3 contiguous HA sequences [3×HA]), which were generously provided by Michel Strubin (4). A NotI-BamHI DNA fragment from pGAL1 HA-H2B encoding ^{HA}H2B was cloned into the doxycycline-regulated pCM188 plasmid (ATCC 87660) by using standard techniques (41). The H3^{HA} gene was amplified from the pGAL1 H3-HA plasmid via PCR using *Pfu* Turbo. The primers used for PCR were designed to incorporate a BamHI or EagI site near the ends of the PCR product. The resulting product, the H3^{HA}-encoding DNA, was cleaved with BamHI and EagI and cloned into the doxycycline-regulated pCM188 plasmid.

To analyze histone density and transcription levels of the *GAL* genes after continuous transcriptional activation, wild-type and *nap1*Δ strains were grown overnight in either yeast extract-peptone (YP)–glucose (2%) medium or YP-galactose (2%) medium, diluted to an optical density at 600 nm (OD_{600}) of ~0.2, and then allowed to undergo 2 cell doublings. When cultures reached an OD_{600} of 0.8 to 1.0, the cells were collected and subjected to chromatin immunoprecipitation (ChIP), immunoblot, or RNA abundance analysis. For the histone exchange experiments, wild-type and *nap1*Δ strains (both in the *bar1*Δ background) were cultured in YP glucose or YP galactose medium continuously (>24 h) to early log phase (OD_{600} = 0.2). α-Factor was then added to the medium to a final concentration of 5 μM, and after 90 to 120 min, cells were arrested in G_1 phase. Shmooing was confirmed visually by using a microscope. Doxycycline was added to a final concentration of 1 μg/ml in YP glucose medium or to a final concentration of 3 μg/ml in YP galactose medium to maintain a consistent histone degradation rate. Following doxycycline treatment, cells were collected every hour for 5 h and subjected to chromatin immunoprecipitation.

Chromatin immunoprecipitation. Chromatin immunoprecipitation (42) assays were performed as previously described (20). The cells were cross-linked with 1% formaldehyde and lysed by bead beating. The cross-liked chromatin was then sheared into small fragments of ~200 bp with sonication. Antibodies and Sepharose beads were added to immunoprecipitate the cross-linked proteins of interest. Cross-linking of the immunoprecipitated material was reversed by incubation overnight at 65°C, and the samples were then treated with proteinase K and RNase A, followed by DNA extraction using the phenol-chloroform method. The isolated DNA was analyzed by quantitative real-time PCR (qPCR). The commercially available antibodies used in this study were anti-H2B (catalog number 39237; Active Motif), anti-H3 (catalog number 1791; Abcam), and anti-HA (catalog number sc-7392; Santa Cruz). ChIP assays were performed in biological triplicates. Unnormalized occupancy was directly calculated from the change in the quantification cycle (ΔC_q) values between the immunoprecipitated DNA and the input control DNA. For the exchange assays, the ratio of the unnormalized HA-tagged histone occupancy over the respective unnormalized total (endogenous plus HA-tagged) histone occupancy at each region for each time point of doxycycline treatment was calculated. The average ratio from three biological replicates at the 0-h time point (T_0) was set as 100% histone persistence, and the average ratios at the remaining time points were calculated as a percentage of histone persistence relative to that at T_0. The histone persistence percentages are shown as means ± standard deviations in Fig. S7 in the supplemental material for comparison between the wt and *nap1*Δ strains. Heat maps (see Fig. 5) were generated by assigning colors to the blocks representing each region during the time course according to the histone persistence percentages. For all other ChIP assays, the total occupancy of each protein at the *GAL* region was normalized to its respective occupancy at a telomere-proximal position (chromosome VI positions 269571 to 269488), which served as the internal control.

RNA abundance. S1 nuclease protection assays to quantify the expression levels of ^{HA}*H2B*, *GAL7*, *GAL10*, *GAL1*, and *tRNA*^{w} were performed as previously described (43). RNA was extracted with the traditional hot-phenol method. For each reaction, ^{32}P-labeled S1 probes were incubated with 40 μg of RNA at 55°C overnight. The hybridized samples were digested by S1 nuclease at 37°C for 30 min and separated by 8% acrylamide sequencing gels. The gels were exposed to phosphor screens, visualized by using a Typhoon PhosphorImager, and analyzed by using ImageQuant software.

Immunoblotting of total protein levels. Cells were harvested at log phase, suspended in lysis buffer (120 mM Tris-HCl [pH 6.8], 12% [vol/vol] glycerol, 3.4% [wt/vol] SDS, 200 mM dithiothreitol [DTT], 0.004% [wt/vol] bromophenol blue), and incubated at 95°C and on ice for 5 min each. Insoluble cell debris was removed by centrifugation, and total protein was separated on a 15% SDS-PAGE gel. The same antibodies against HA, H2B, and H3 that were used for ChIP analysis were used for protein detection. For the quantification of total protein levels during histone exchange, the protein level of each strain at T_0 was set as 100%; the protein levels at the remaining time points were calculated as a percentage relative to that at T_0.

***In vitro* H2A-H2B dimer-binding competition assay.** Förster resonance energy transfer (FRET)-based competition assays were conducted in a 384-well format using Alexa Fluor 488-labeled *Xenopus laevis* histone H2A-H2B (with a threonine 118-to-cysteine mutation in H2B for labeling purposes) as described previously (44). The final reaction buffer contained 20 mM Tris-HCl (pH 7.5), 300 mM NaCl, 5% (vol/vol) glycerol, 0.01% (vol/vol) NP-40, 0.01% (vol/vol) 3-[(3-cholamidopropyl)-dimethylammonio]-1-propanesulfonate (CHAPS), 1 mM DTT, and 1 mM EDTA (pH 8.0), and the reaction volume was 40 μl. Each PCR-prepared fragment was titrated against 10 nM histone H2A-H2B in the presence 50 nM 59-bp DNA. Each reaction was performed in duplicate, and control titrations containing only one labeled component were used to correct the raw FRET signal to produce $FRET_{corrected}$. Each experiment contained an internal control titration of recombinant 147-bp Widom 601 DNA (data not shown). Reaction mixtures were pipetted into a microplate and scanned by using a Typhoon Trio variable-mode imager (GE). Three scans were performed, using excitation/emission wavelengths of 488/520 nm, 633/670 nm, or 488/670 nm. Fluorescence was quantified by using ImageQuant software. *GAL* fragment titration produced a sigmoidal curve from which a 50% inhibitory concentration (IC_{50}) was determined by using GraphPad Prism software. Data were normalized and fit to have a minimum of 0 and a maximum of 100%. At least two independent titrations were performed for each fragment, and all IC_{50} values used in the mean calculation were derived from data with an R^2 of >0.98.

***In vitro* micrococcal nuclease analysis of chromatin.** *In vitro* micrococcal nuclease (MNase) digestion assays were performed according to established protocols (45). Canonical mononucleosomes and trinucleosomes were reconstituted by salt dilution using a purified recombinant *Xenopus laevis* octamer on a 207-bp DNA fragment containing the 147-bp Widom 601 nucleosome-positioning sequence with 30 bp of flanking linker DNA (46). Nucleosomal DNA or free DNA (5 μg; 0.17 μM) was used for each MNase digestion. MNase digestion was performed in the

absence and presence of excess recombinant *Xenopus laevis* histone H2A/H2B dimer. A 3-fold molar excess of histone H2A-H2B dimer was added to a final concentration of 0.51 μM, and the mixture was incubated for 5 min, followed by MNase digestion at room temperature for the indicated times. Reactions were quenched with EDTA to a final concentration of 12.5 mM. The DNA was purified by the addition of SDS (0.5%) and proteinase K (0.2 mg/ml), and the mixture was incubated at 50°C for 30 min, phenol-chloroform extracted, and ethanol precipitated. The samples were separated on a 6% native polyacrylamide gel and stained with SYBR gold.

Micrococcal nuclease analysis of chromatin structure *in vivo*. Detailed protocols for micrococcal nuclease analysis of the chromatin structure *in vivo* can be found in the supplemental material. Nuclei were isolated from wild-type (BY4741) and *nap1*Δ cells essentially as described previously (47). Indirect end-labeling analysis was completed as described previously (24), and primer extension analysis was performed as described previously (48). The membranes and gels were exposed to phosphor storage screens, visualized on a Typhoon PhosphorImager, and quantitated by using ImageQuant TL software.

Reconstitution studies of *GAL* fragments. Nucleosome reconstitution was performed by using the salt dilution method (49). *Xenopus laevis* histone octamers were titrated against each PCR-prepared DNA fragment. Reaction mixtures were separated on 5% native gels, stained with ethidium bromide, and visualized by UV.

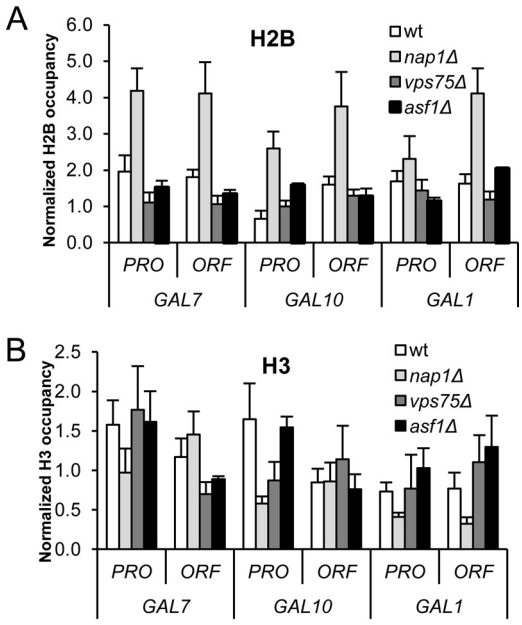

FIG 1 Excess H2A-H2B accumulation is observed with loss of Nap1 but not Vps75 or Asf1. Shown is the occupancy of histone H2B (A) or histone H3 (B) at the *GAL* locus under transcriptionally repressed conditions (glucose) in the wild-type (wt), *nap1*Δ, *vps75*Δ, and *asf1*Δ strains as determined by ChIP assays. Data are represented as the means from 3 biological replicates ± standard deviations, normalized to the levels of occupancy at a telomere-proximal location.

RESULTS

Nap1 prevents excess histone H2A-H2B accumulation on linker DNA. We previously showed that a knockout of the histone chaperone *NAP1* in *S. cerevisiae* results in an atypical chromatin structure with excess H2A-H2B at most positions across the *GAL* locus (20). We next asked whether this was a general feature of Nap family proteins by assaying a strain deleted for Vps75, a histone chaperone with a structure similar to that of Nap1 (50). We utilized chromatin immunoprecipitation (ChIP) assays to visualize H2A-H2B (via H2B) and H3-H4 (via H3) occupancy at six different regions of the *GAL* locus. The relative positions of the sites were selected based on extensive studies of nucleosome positioning, histone density, and histone variant H2A.Z occupancy (51–55) and include three promoter (PRO) and three open reading frame (ORF) sites (see Fig. S1 in the supplemental material). The *GAL10* and *GAL1* genes are divergently transcribed and share one upstream activating sequence (UAS) (23, 56, 57). As shown previously (20), loss of Nap1 (*nap1*Δ) causes a general increase in the level of H2A-H2B compared to that in the wild-type strain at all sites but one (Fig. 1A). At these sites, the occupancy of H3-H4 remains at or slightly below wild-type levels (Fig. 1B). In contrast, deletion of *VPS75* (*vps75*Δ) does not significantly change H2A-H2B or H3-H4 occupancy across the *GAL* locus. We also deleted *ASF1* (*asf1*Δ), a histone chaperone structurally distinct from Nap1 and Vps75 (58), and detected no significant changes in H2A-H2B or H3-H4 occupancy. Thus, excess H2A-H2B accumulation is not a shared feature of strains deleted for Nap family proteins or other histone chaperones but is unique to the *nap1*Δ strain. Together, these data indicate that preventing this atypical chromatin is a unique function of Nap1.

We next characterized chromatin with H2A-H2B enrichment biochemically. To mimic the atypical chromatin observed *in vivo* in the *nap1*Δ strain, mononucleosomes were incubated in the presence (and absence) of excess H2A-H2B, and the micrococcal nuclease (MNase) digestion patterns were compared (Fig. 2A). We used a 207-bp DNA fragment carrying the well-characterized 147-bp Widom 601 nucleosome-positioning sequence (59) and 30 bp of flanking linker DNA. As expected, free DNA was rapidly digested by MNase. Incubation of DNA with H2A-H2B resulted in modest protection from MNase. A clearly defined protected region was not observed, consistent with the nonspecific binding of H2A-H2B to DNA. MNase digestion of mononucleosomes revealed a well-defined 140- to 180-bp region (depending on the digestion time) of protection, indicating that the linker DNA is digested more rapidly than nucleosomal DNA (45). Mononucleosomes with excess H2A-H2B displayed significantly increased resistance to MNase digestion and broader DNA protection surrounding the nucleosome site. This suggests that excess H2A-H2B binds to the flanking linker DNA.

We also performed MNase digestion assays on two other nucleosome templates: a 621-bp DNA fragment capable of forming trinucleosomes with three consecutive 207-bp Widom 601 nucleosome-positioning sequences with linker DNA (see Fig. S2A in the supplemental material) and a 588-bp native promoter DNA fragment without detectable positioning sequences (60) (see Fig. S2B in the supplemental material). Similar results were observed for all DNA fragments: the addition of excess H2A-H2B to reconstituted nucleosomes significantly increased resistance to MNase digestion. These results indicate that excess H2A-H2B binds to linker DNA in the context of both mono- and multinucleosome templates.

We next assayed how excess H2A-H2B affects chromatin architecture *in vivo* by measuring MNase digestion patterns of chromatin from wild-type and *nap1*Δ cells. Cleavage patterns within the *GAL* locus were assessed by high-resolution (single-base-pair) reiterative primer extension analysis. The *GAL1* and *GAL10* promoters were analyzed, since the *GAL1* promoter had normal levels

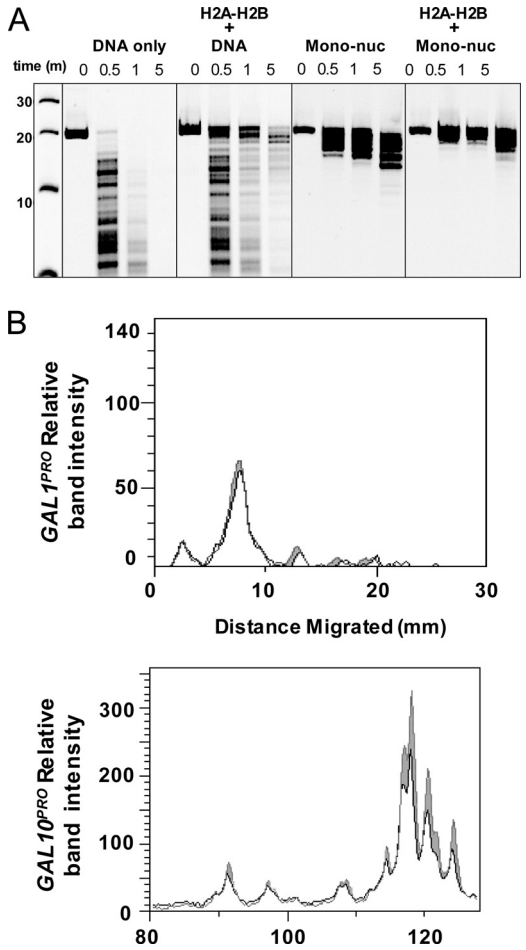

FIG 2 H2A-H2B accumulation protects DNA from MNase digestion. (A) *In vitro* analysis of chromatin with and without excess H2A-H2B. Shown are data from PAGE analysis of MNase digestion of naked DNA alone, DNA with H2A-H2B, mononucleosomes (Mono-nuc), and mononucleosomes with H2A-H2B, assessed on a 207-bp DNA fragment. (B) Chromatin from wild-type and *nap1*Δ cells was digested with MNase *in vivo*, and the cleavage products were analyzed by primer extension assays. Quantitation of the primer extension products from the *GAL1* promoter (top) and the *GAL10* promoter (bottom) is shown in black for *nap1*Δ cells and in gray for wild-type cells. The *GAL10* promoter, which has excess H2A-H2B as determined by ChIP assays, is more protected from MNase cleavage in *nap1*Δ cells.

and the *GAL10* promoter had excess levels of H2A-H2B in the *nap1*Δ strain as determined by ChIP analysis (Fig. 1). As expected, at the *GAL1* promoter, there were no differences observed in the MNase digestion patterns of chromatin from wild-type and *nap1*Δ cells (Fig. 2B; see also Fig. S3A in the supplemental material). The *GAL10* promoter region is hypersensitive to MNase cleavage, and this is reflected in the amount of product that terminates within the hypersensitive region (Fig. 2B; see also Fig. S3B in the supplemental material). Although subtle, MNase cleavage of the chromatin from *nap1*Δ cells is reproducibly reduced in the region of *GAL10* that exhibits excess H2A-H2B by ChIP analysis compared to the chromatin from wild-type cells. The minor reduction in MNase cleavage is not unexpected. Nucleosomes in the *GAL* locus evaluated at high resolution in fact occupy multiple positions (36). Thus, the excess dimer is most likely binding at multiple positions, leading to the subtle difference seen in the primer extension products. Taken together, the *in vitro* and *in vivo* MNase results suggest that the excess H2A-H2B is binding to the linker DNA.

Occupancy of the histone variant H2A.Z is unchanged in the *nap1*Δ strain. Histone H2A.Z (Htz1 in yeast) is a variant of histone H2A that substitutes for the canonical major histone H2A in a wide, but nonrandom, genomic distribution (61). H2A.Z is involved in transcription regulation, gene activation and silencing, DNA repair, and chromosomal stability (62). Since Nap1 also interacts with H2A.Z (63), we investigated whether the occupancy of H2A.Z is altered in the absence of Nap1. Chromatin tandem affinity purification (TAP) was performed by using TAP-tagged Htz1 (Htz1-TAP) in the wild-type or *nap1*Δ strain with analyses of the *GAL* locus genes. In wild-type cells, significant occupancy of Htz1 was detected across the region, and this occupancy was unaffected by the loss of Nap1 (see Fig. S4 in the supplemental material). These results indicate that Nap1 is not required for normal levels of Htz1 occupancy at these specific regions, nor does Htz1 accumulate in the same manner as major H2A in this region in the absence of Nap1.

Histone H2A-H2B accumulation in the *nap1*Δ strain is independent of DNA sequence. The various degrees of H2A-H2B accumulation across the *GAL* locus in *nap1*Δ cells (Fig. 1) prompted us to test the role of DNA sequence. Some studies suggest that DNA sequence is a major factor in nucleosome positioning (64, 65), while others argue that it may be only a partial factor (66–69). To test the role of sequence *in vitro*, we used a Förster resonance energy transfer (FRET) competition assay (44) to compare H2A-H2B affinities for the six different *GAL* promoter (PRO) and open reading frame (ORF) sequences, all of ~150 bp. We first measured FRET of a complex between H2A-H2B and a 59-bp DNA fragment containing the H2A-H2B-binding region of the well-characterized Widom 601 nucleosome-positioning sequence (59). We titrated each of the *GAL* locus DNAs and measured the half-maximal inhibitory concentration (IC_{50}) values as the FRET signal decreased to zero (Fig. 3A). A lower IC_{50} reflects a lower dissociation constant (K_d) or a tighter interaction between the *GAL* locus DNA and H2A-H2B. All *GAL* locus DNAs were able to fully compete with the 59-bp DNA for H2A-H2B, indicating efficient H2A-H2B-*GAL* DNA interactions. Slight differences in IC_{50}s were observed among the *GAL* DNAs (10 to 30 nM), which did not correlate with H2A-H2B accumulation in *nap1*Δ cells. For example, the lowest IC_{50} was measured with the $GAL10^{PRO}$ and $GAL1^{PRO}$ DNAs, which in fact possessed the highest and lowest levels, respectively, of H2A-H2B accumulation *in vivo*. We noticed, however, that the *in vitro* binding of H2A-H2B correlates with the DNA GC content (Fig. 3B). DNA with a lower CG content is more flexible (70), consistent with the lower K_d for H2A-H2B binding. Overall, these data indicate that the DNA sequences themselves do not account for the varied H2A-H2B accumulation across the *GAL* locus in the absence of Nap1 *in vivo*. This implies the involvement of other extrinsic factors.

Transcription removes accumulated histone H2A-H2B in the *nap1*Δ strain. The above-mentioned accumulation of H2A-H2B in the *nap1*Δ strain was observed under repressed conditions for *GAL* gene expression (glucose medium). We next asked if this atypical H2A-H2B distribution remained when the *GAL* genes were actively transcribed. Histone occupancy was assayed by using ChIP after growth under inducing conditions (galactose medium) for 24 h or ~10 generations. The ratio of H2A-H2B occupancy (H2B) to H3-H4 occupancy (H3) at each location revealed no

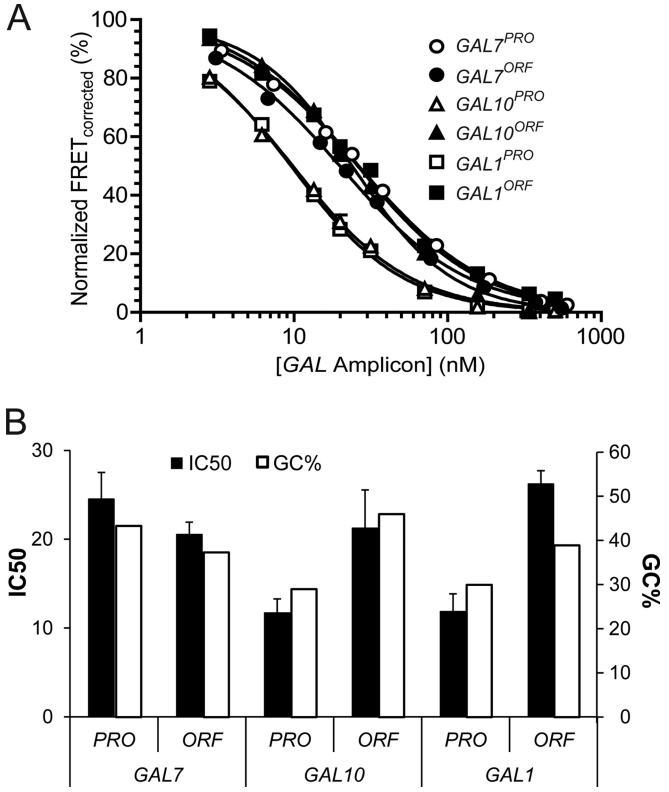

FIG 3 All six *GAL* DNA fragments bind histone H2A-H2B with comparable affinities. H2A-H2B-DNA-binding affinities were measured with a FRET-based competition assay. DNA fragments (~150 bp) from the six promoter (PRO) and open reading frame (ORF) sites of *GAL7*, *GAL10*, and *GAL1* were titrated in the presence of 50 nM the 59-bp dimer-binding region of the 601 sequence and analyzed for binding to Alexa Fluor 488-labeled histone H2A-H2B. (A) Representative competition curves. Each data point reflects the mean of results from duplicate measurements ± 1 standard error of the mean. The errors bars are small and in many cases not visible. All curves used for statistics had an R^2 value of ≥0.98. (B) Mean IC_{50} values for at least 2 replicates and percent GC contents for the DNA sequences. Error bars reflect 1 standard error of the mean.

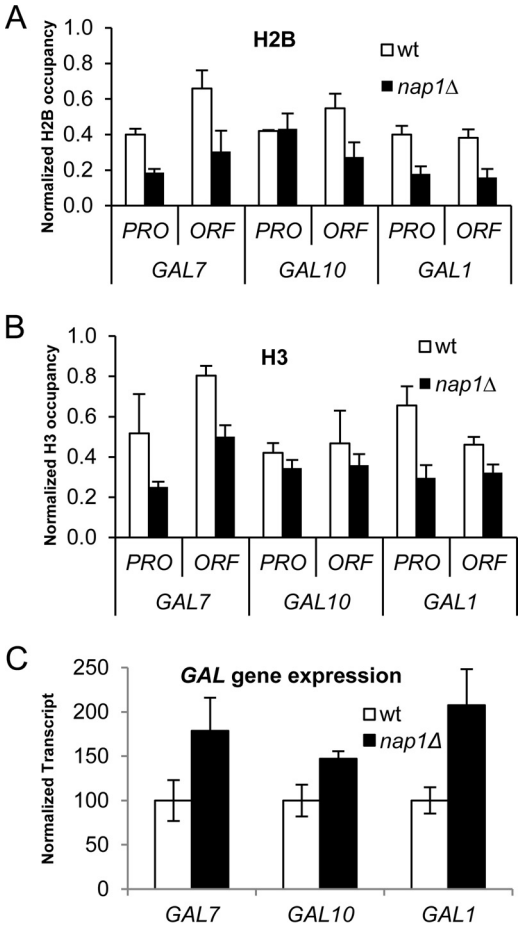

FIG 4 H2A-H2B accumulation is not maintained in the *nap1*Δ strain at the *GAL* locus under induced conditions. (A and B) The occupancies of H2B (A) or H3 (B) in the wt strain and the *nap1*Δ strain under active transcription were determined by ChIP assays. (C) Transcript levels of *GAL* genes in the wt and *nap1*Δ strains were detected by S1 nuclease protection assays with ^{32}P-labeled probes specific to *GAL7*, *GAL10*, *GAL1*, and *tRNA^w*. The transcript levels of *tRNA^w* were used as an internal control for normalization. Bars reflect the means from 3 biological replicates ± standard deviations.

significant difference between the wild-type and *nap1*Δ strains or between different *GAL* loci (Fig. 4A and B; see also Fig. S5A in the supplemental material). This indicates that excess H2A-H2B does not stably accumulate during active transcription. It is important to note, however, that the occupancies of both H2B and H3 were lower in the *nap1*Δ strain than in the wild type at every site tested except *GAL10^{PRO}*, where the occupancy in the *nap1*Δ strain was similar to that in the wild type. Analysis of extracts confirmed that this decrease in histone occupancy is not due to lower overall levels of histones in the *nap1*Δ strain (see Fig. S5B in the supplemental material). The lower nucleosome occupancy in galactose in cells lacking Nap1 thus reflects a change in histone deposition, supporting a nucleosome assembly role for Nap1. Since the transcribing *GAL* locus in the *nap1*Δ strain has lower histone occupancy, we tested whether this impacted gene expression using S1 nuclease protection assays (Fig. 4C). High expression levels were observed from the *GAL* genes in *nap1*Δ cells relative to the wild-type strain. Thus, the reduced histone density at the *GAL* locus observed in the absence of Nap1 is linked to increased transcription levels, implicating Nap1 in the repression of gene expression via maintenance of histone occupancy, potentially through nucleosome assembly *in vivo*.

Establishment of an *in vivo* doxycycline-regulated histone exchange system. To further investigate the role of Nap1, we developed a method to measure histone exchange at the *GAL* locus. We created an *in vivo* system in which the expression of epitope-tagged histones is controlled by using doxycycline (Fig. 5A). Previously reported histone exchange studies utilized a system in which tagged histone expression is *GAL* promoter regulated and therefore induced by the presence of galactose (4–9). Since we wanted to evaluate histone exchange specifically at the *GAL* locus, we needed a different means to control histone expression. We subcloned HA-tagged versions of histones H2B (^{HA}H2B) and H3 (H3^{HA}) (4) into a doxycycline-controlled expression vector. In this system, expression of the HA-tagged histones is repressed when doxycycline is present. These plasmids were introduced into both the wild-type and *nap1*Δ strains, in a *bar1*Δ background. The *bar1*Δ background increases α-factor sensitivity, which arrests cells in G_1 (39), such that subsequent studies are replication independent. As expected, the addition of doxycycline resulted in transcriptional repression of the HA-tagged histone and did not affect

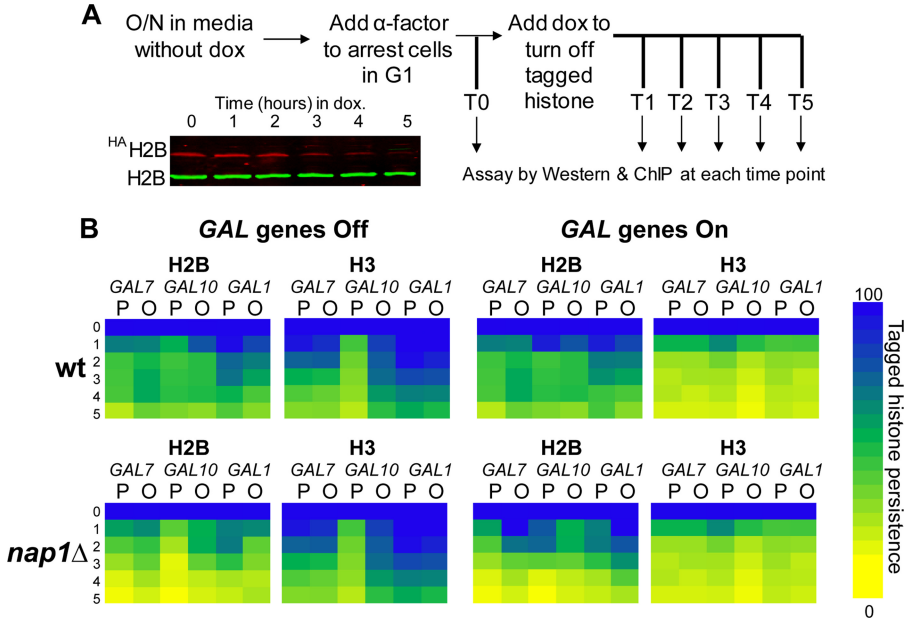

FIG 5 Histone exchange rates at the *GAL* locus are distinct, and Nap1 is involved in H2A-H2B exchange. (A) Schematic of histone exchange assays with a representative Western blot showing decreasing HA-tagged H2B levels and unchanged endogenous H2B levels. O/N, overnight; dox, doxycycline. (B) Heat maps showing tagged histone persistence over the 5-h time course. Persistence is defined as the percentage of tagged histone occupancy (detected with anti-HA) over endogenous histone occupancy (detected with anti-H3) under transcriptionally repressed ("Off") or activated ("On") conditions in the wt and *nap1*Δ strains. The tagged histone persistence at T_0 was set as 100% (dark blue). Bright yellow indicates that tagged histone was completely exchanged (0% tagged histone persistence). Promoter (P) and ORF (O) regions are indicated.

GAL gene expression in either wild-type or *nap1*Δ cells (see Fig. S6 in the supplemental material). After the addition of doxycycline, the level of total H2B protein (endogenous plus ^{HA}H2B, detected by anti-H2B antibody) was not affected, whereas the level of ^{HA}H2B protein (detected by anti-HA antibody) gradually diminished (see Fig. S7A and B in the supplemental material). After 5 h of repression by doxycycline, the ^{HA}H2B level dropped to <20% of the predoxycycline levels, with no impact on endogenous histone levels.

We next utilized ChIP assays to measure the occupancy of ^{HA}H2B and total H2B at a telomere-proximal location as a standard for the assay. H2B exchange was observed at this location (see Fig. S7C and D in the supplemental material). During the 5 h following doxycycline addition, the decrease in ^{HA}H2B protein levels correlated directly with the decrease in ^{HA}H2B occupancy, whereas the occupancy of total H2B was not affected by doxycycline treatment. Histone exchange data for the telomere-proximal control region with doxycycline-regulated H3^{HA} were similar to those obtained with ^{HA}H2B (data not shown), and it is important to note that neither H2B (tagged or untagged) nor H3 (tagged or untagged) levels were impacted by the deletion of Nap1 (see Fig. S8 in the supplemental material).

Histone exchange rates vary across the *GAL* locus. We utilized the doxycycline-regulated histone exchange system to determine exchange rates at the *GAL* locus. We tested both wild-type and *nap1*Δ strains and compared them under repressed and transcriptionally active conditions (Fig. 5B). To visualize and compare the complex histone exchange patterns at the different *GAL* loci, the percentage of HA-tagged histone that persists at each site is shown as a heat map. Under transcriptionally repressed conditions, exchange of both H2B and H3 was observed in the wild-type strain at all promoter and open reading frame sites tested (Fig. 6A and B). However, the exchange kinetics differ, depending on the site. Histone H2B exchange is the least dynamic at $GAL1^{PRO}$ and $GAL1^{ORF}$, where the exchange rate is similar to the exchange rate at the telomere-proximal region. The most dynamic exchange was observed at $GAL10^{PRO}$, where persistence of the tagged derivative was down to 50% within an hour. In general, H2B exchange is significantly more dynamic than H3 exchange across the *GAL* locus, a trend that was also shown in a previous study (4). The one exception to this trend is $GAL10^{PRO}$, where the exchange of H3 is as dynamic as that of H2B. The rapid exchange of both H2A-H2B and H3-H4 at $GAL10^{PRO}$ indicates a highly dynamic chromatin structure at this location, even when transcription is off. Under transcriptionally repressed conditions, there was very little impact of the loss of Nap1 on histone H2B or H3 exchange at the promoter and open reading frame of all *GAL* sites tested, except for a decrease in the exchange of H2B at the otherwise highly dynamic $GAL10^{PRO}$ site. The absence of Nap1 reduces H2B exchange but does not affect H3 exchange. This indicates that the "old" or tagged version of H2B is being reassembled into chromatin in the absence of Nap1. This suggests that when present, Nap1 facilitates the incorporation of "new" histones and not the reassembly of the old histones, at least at this highly dynamic position. It is important to note that these studies were performed with cell cycle-arrested cells, so this Nap1 function is independent of histone deposition during replication.

When *GAL* gene transcription was activated, the exchange kinetics of both H2B and H3 in the wild-type strain were highly dynamic across the locus (Fig. 5 and 6C and D), to a level comparable to that of $GAL10^{PRO}$ in the absence of transcription. This rapid transcription-mediated histone exchange is consistent with

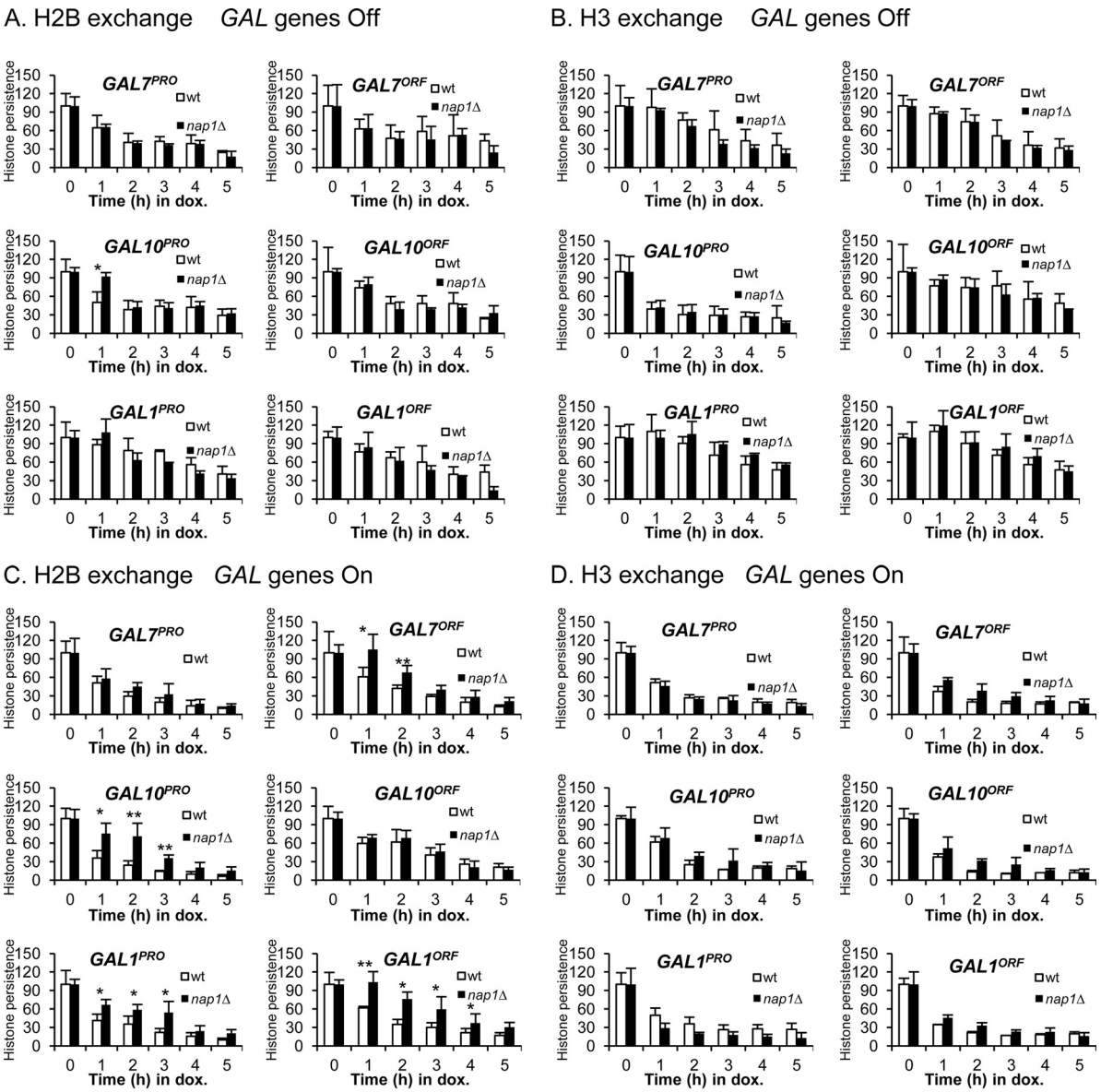

FIG 6 Histone persistence varies depending upon the time of shutoff and the specific *GAL* region. Histone persistence is defined as the relative percentage of tagged histone occupancy (detected with anti-HA) over endogenous histone occupancy (detected with anti-H2B or anti-H3) under *GAL* gene transcriptionally repressed ("Off") or activated ("On") conditions in the wt and *nap1*Δ strains. The histone persistence at T_0 was set as 100%. (A and B) H2B (A) and H3 (B) persistence at the *GAL* locus under transcriptionally repressed conditions. (C and D) H2B (C) and H3 (D) persistence under continuous transcriptionally active conditions. P, promoter; O, ORF. *, *P* value of <0.05; **, *P* value of <0.01.

previously reported observations that nucleosomes are highly dynamic at the *GAL* locus upon the activation of transcription (20, 25, 30, 31, 71). In the *nap1*Δ strain, H2B exchange kinetics were less dynamic across the region, whereas histone H3 exchange was similar to that of the wild type (Fig. 6C and D). Therefore, when transcription is active and chromatin is highly dynamic in the wild-type strain, H2A-H2B exchange is consistently slower in the absence of Nap1.

***In vitro* nucleosome reconstitution recapitulates some of the *in vivo* dynamics of the *GAL* locus.** The various regions of the *GAL* locus exhibit distinctive exchange profiles in the wild-type strain (Fig. 5B). Since DNA sequence can directly affect nucleosome stability and contribute to *in vivo* nucleosome dynamics (64, 65), we tested the fragments for their intrinsic ability to form nucleosomes. Using the 601 positioning sequence (59) as a control, the *GAL* fragments were analyzed for the formation of stable, positioned nucleosomes by salt reconstitution with native histones (49) (see Fig. S9 in the supplemental material). This allowed us to group the *GAL* fragments into three classes, represented by 601 (601 and $GAL7^{ORF}$), the *GAL10* promoter ($GAL10^{PRO}$, $GAL10^{ORF}$, and $GAL7^{PRO}$), and the *GAL1* promoter ($GAL1^{PRO}$ and $GAL1^{ORF}$). In some cases, multiple forms of DNA-histone complexes were evident. To identify the histone composition of the complexes, nucleosome reconstitution was performed with fluorescently labeled histones (see Fig. S10 in the supplemental material). In addition, heat-shifting and lower-salt experiments

were used to determine if complexes were well positioned (see Fig. S11 in the supplemental material). The results indicate that the 601 class forms hexasomes and positioned nucleosomes at low concentrations of the octamer, with an increase in the amount of nucleosomes as the octamer is titrated. The *GAL1* promoter class formed stable, positioned nucleosomes more efficiently than did 601, in that only a single band was observed even at low octamer levels. Both of the fragments in this class (*GAL1* promoter and *GAL1* ORF) had the least dynamic nucleosomes *in vivo* in the exchange assay for both H2B and H3, suggesting that sequence plays an important role in these properties. The *GAL10* promoter class formed intermediate complexes and different forms of nucleosomes at every ratio *in vitro*, suggesting that nucleosomes are not stable and/or that there are multiple nucleosome positions. The *GAL10* promoter region was the highly dynamic site in the *in vivo* exchange assay (Fig. 5), but the other two fragments in this unstable *in vitro* class (*GAL10* ORF and *GAL7* promoter) did not share this behavior *in vivo*.

DISCUSSION

We previously found that Nap1 prevents the formation of atypical chromatin characterized by excess H2A-H2B across the *GAL* locus under transcriptionally repressed conditions (20). Here, we show that H2A-H2B accumulation does not occur in a strain deleted for the Nap1 family member Vps75 or the H3-H4 histone chaperone Asf1. In addition, this effect is specific for the major histone variants, as H2A.Z does not accumulate in these same regions. Although H2A-H2B accumulation varies at different locations in the absence of Nap1, we found this is not likely due to variable H2A-H2B-DNA binding, as *in vitro* affinities did not correlate with *in vivo* accumulation. The excess H2A-H2B appears to bind between nucleosomes in the linker regions, as evidenced by *in vitro* and *in vivo* MNase protection assays. Notably, the process of transcription results in a loss of the excess H2A-H2B, and in fact, the absence of Nap1 leads to lower overall histone density on chromatin, indicative of critical nucleosome assembly functions of Nap1.

Nucleosomal histones are readily exchanged into and out of chromatin (4, 5). This histone exchange is a combination of partial nucleosome disassembly and reassembly, and histone chaperones are directly involved in this process (3, 7, 8, 72–74). However, studies on the requirement for histone chaperones in histone exchange within nucleosomes have focused primarily on H3-H4 histone chaperones (7, 9, 75). Also, most histone exchange studies utilize a galactose-inducible promoter for the regulation of tagged histone expression (4–9); therefore, *GAL* locus gene transcription is affected when the expression of the tagged histones is turned on or off. In this study, we designed a doxycycline-regulated histone exchange system that does not affect *GAL* gene transcription. Histone exchange is generally observed across the *GAL* locus under repressed conditions, with the exchange of both H2B and H3 being highly dynamic at the *GAL10* promoter ($GAL10^{PRO}$). Furthermore, the highly dynamic H2B exchange is Nap1 dependent, whereas H3 exchange is not. It is intriguing that even without active transcription, the nucleosome at the *GAL10* promoter is highly dynamic. One unique feature of the chromatin at this site is a lower H2B occupancy in general; the *GAL10* promoter has only half the H2B occupancy of other *GAL* sites (20). Moreover, in the absence of Nap1, this decrease in H2B occupancy is reversed (20), and the H2A-H2B exchange rate is severely reduced. Importantly, the *GAL10* promoter region has the binding site for the Gal4-Gal80 activator complex and the RSC chromatin-remodeling complex under transcriptionally repressed conditions (55). *In vitro* studies have shown that RSC promotes histone transfer (76). In the presence of Nap1, RSC releases one H2A-H2B from the nucleosome to form a hexasome, and the dimer is transferred to Nap1 (19). This combination of highly dynamic Nap1-dependent H2A-H2B exchange, a 2-fold reduction in H2B occupancy, and the presence of an RSC-binding site supports a model whereby hexasome formation likely occurs at the *GAL10* promoter *in vivo*.

Taken together, the findings presented here advance our understanding of the diverse roles of the histone chaperone Nap1 in chromatin regulation *in vivo* (see Fig. S12 in the supplemental material): (i) removal of atypical histone H2A-H2B under transcriptionally repressed conditions, (ii) maintenance of proper histone density on chromatin during activated transcription (i.e., transcription-coupled assembly), and (iii) facilitation of histone H2A-H2B exchange within highly dynamic chromatin regions whether the locus is repressed or activated. The active exchange of H2A-H2B could lead to the destabilization of the H3-H4 tetramer; thereby, Nap1 could also contribute to nucleosome disassembly. This is consistent with the findings that deletion of *NAP1* reverses the cryptic transcript phenotype (interpreted as the by-product of underassembled chromatin) observed in mutant strains defective for other chromatin regulators (77) and that Nap1 has an important function in the eviction of histones during transcription in a mammalian *in vitro* system (17). Importantly, these varied functions of Nap1 are not redundant with other histone chaperones *in vivo*. Since Nap1 has a high affinity for H3-H4 tetramers as well as H2A-H2B dimers (14), Nap1 has the potential to function independently in these various roles. However, a large body of work indicates collaborative functional activities between Nap1 and other chaperones as well as ATP-dependent chromatin remodelers and histone acetyltransferases (13, 17–19, 60, 77–79). How the combinatorial action of these factors contributes to histone occupancy and dynamics *in vivo* remains to be elucidated.

ACKNOWLEDGMENTS

Plasmids with tagged histones were kind gifts from Michel Strubin. We thank the Protein Expression and Purification (PEP) Facility at Colorado State University for purified histones and Kyle W. Martin for assistance with the FRET assays.

FUNDING INFORMATION

HHS | NIH | National Institute of General Medical Sciences (NIGMS) provided funding to Xu Chen, Sheena D'Arcy, Catherine A. Radebaugh, Daniel D. Krzizike, Holli A. Giebler, Jennifer Nyborg, Karolin Luger, and Laurie A. Stargell under grant number P01 GM088409. Howard Hughes Medical Institute (HHMI) provided funding to Sheena D'Arcy, Daniel D. Krzizike, and Karolin Luger. NSF | BIO | Division of Molecular and Cellular Biosciences (MCB) provided funding to Liangquan Huang and Laurie A. Stargell under grant number 1330019.

The funding agencies had no role in study design, data collection and interpretation, or the decision to submit the work for publication.

REFERENCES

1. **Luger K, Mader AW, Richmond RK, Sargent DF, Richmond TJ.** 1997. Crystal structure of the nucleosome core particle at 2.8 A resolution. Nature **389:**251–260. http://dx.doi.org/10.1038/38444.
2. **Luger K, Dechassa ML, Tremethick DJ.** 2012. New insights into nucleosome and chromatin structure: an ordered state or a disordered affair? Nat Rev Mol Cell Biol **13:**436–447. http://dx.doi.org/10.1038/nrm3382.
3. **Linger J, Tyler JK.** 2006. Global replication-independent histone H4

exchange in budding yeast. Eukaryot Cell **5:**1780–1787. http://dx.doi.org/10.1128/EC.00202-06.
4. **Jamai A, Imoberdorf RM, Strubin M.** 2007. Continuous histone H2B and transcription-dependent histone H3 exchange in yeast cells outside of replication. Mol Cell **25:**345–355. http://dx.doi.org/10.1016/j.molcel.2007.01.019.
5. **Dion MF, Kaplan T, Kim M, Buratowski S, Friedman N, Rando OJ.** 2007. Dynamics of replication-independent histone turnover in budding yeast. Science **315:**1405–1408. http://dx.doi.org/10.1126/science.1134053.
6. **Rufiange A, Jacques PE, Bhat W, Robert F, Nourani A.** 2007. Genome-wide replication-independent histone H3 exchange occurs predominantly at promoters and implicates H3 K56 acetylation and Asf1. Mol Cell **27:**393–405. http://dx.doi.org/10.1016/j.molcel.2007.07.011.
7. **Kim HJ, Seol JH, Han JW, Youn HD, Cho EJ.** 2007. Histone chaperones regulate histone exchange during transcription. EMBO J **26:**4467–4474. http://dx.doi.org/10.1038/sj.emboj.7601870.
8. **Gat-Viks I, Vingron M.** 2009. Evidence for gene-specific rather than transcription rate-dependent histone H3 exchange in yeast coding regions. PLoS Comput Biol **5:**e1000282. http://dx.doi.org/10.1371/journal.pcbi.1000282.
9. **Jamai A, Puglisi A, Strubin M.** 2009. Histone chaperone spt16 promotes redeposition of the original h3-h4 histones evicted by elongating RNA polymerase. Mol Cell **35:**377–383. http://dx.doi.org/10.1016/j.molcel.2009.07.001.
10. **van Bakel H, Tsui K, Gebbia M, Mnaimneh S, Hughes TR, Nislow C.** 2013. A compendium of nucleosome and transcript profiles reveals determinants of chromatin architecture and transcription. PLoS Genet **9:**e1003479. http://dx.doi.org/10.1371/journal.pgen.1003479.
11. **Loyola A, Almouzni G.** 2004. Histone chaperones, a supporting role in the limelight. Biochim Biophys Acta **1677:**3–11. http://dx.doi.org/10.1016/j.bbaexp.2003.09.012.
12. **Park YJ, Luger K.** 2006. Structure and function of nucleosome assembly proteins. Biochem Cell Biol **84:**549–558. http://dx.doi.org/10.1139/o06-088.
13. **Zlatanova J, Seebart C, Tomschik M.** 2007. Nap1: taking a closer look at a juggler protein of extraordinary skills. FASEB J **21:**1294–1310. http://dx.doi.org/10.1096/fj.06-7199rev.
14. **Andrews AJ, Downing G, Brown K, Park YJ, Luger K.** 2008. A thermodynamic model for Nap1-histone interactions. J Biol Chem **283:**32412–32418. http://dx.doi.org/10.1074/jbc.M805918200.
15. **D'Arcy S, Martin KW, Panchenko T, Chen X, Bergeron S, Stargell LA, Black BE, Luger K.** 2013. Chaperone Nap1 shields histone surfaces used in a nucleosome and can put H2A-H2B in an unconventional tetrameric form. Mol Cell **51:**662–677. http://dx.doi.org/10.1016/j.molcel.2013.07.015.
16. **Fujii-Nakata T, Ishimi Y, Okuda A, Kikuchi A.** 1992. Functional analysis of nucleosome assembly protein, NAP-1. The negatively charged COOH-terminal region is not necessary for the intrinsic assembly activity. J Biol Chem **267:**20980–20986.
17. **Luebben WR, Sharma N, Nyborg JK.** 2010. Nucleosome eviction and activated transcription require p300 acetylation of histone H3 lysine 14. Proc Natl Acad Sci U S A **107:**19254–19259. http://dx.doi.org/10.1073/pnas.1009650107.
18. **Lorch Y, Maier-Davis B, Kornberg RD.** 2006. Chromatin remodeling by nucleosome disassembly in vitro. Proc Natl Acad Sci U S A **103:**3090–3093. http://dx.doi.org/10.1073/pnas.0511050103.
19. **Kuryan BG, Kim J, Tran NN, Lombardo SR, Venkatesh S, Workman JL, Carey M.** 2012. Histone density is maintained during transcription mediated by the chromatin remodeler RSC and histone chaperone NAP1 in vitro. Proc Natl Acad Sci U S A **109:**1931–1936. http://dx.doi.org/10.1073/pnas.1109994109.
20. **Andrews AJ, Chen X, Zevin A, Stargell LA, Luger K.** 2010. The histone chaperone Nap1 promotes nucleosome assembly by eliminating non-nucleosomal histone DNA interactions. Mol Cell **37:**834–842. http://dx.doi.org/10.1016/j.molcel.2010.01.037.
21. **Citron BA, Donelson JE.** 1984. Sequence of the *Saccharomyces GAL* region and its transcription in vivo. J Bacteriol **158:**269–278.
22. **Lohr D, Venkov P, Zlatanova J.** 1995. Transcriptional regulation in the yeast *GAL* gene family: a complex genetic network. FASEB J **9:**777–787.
23. **Lohr D, Hopper JE.** 1985. The relationship of regulatory proteins and DNaseI hypersensitive sites in the yeast *GAL1-10* genes. Nucleic Acids Res **13:**8409–8423. http://dx.doi.org/10.1093/nar/13.23.8409.
24. **Cavalli G, Thoma F.** 1993. Chromatin transitions during activation and repression of galactose-regulated genes in yeast. EMBO J **12:**4603–4613.
25. **Han M, Grunstein M.** 1988. Nucleosome loss activates yeast downstream promoters in vivo. Cell **55:**1137–1145. http://dx.doi.org/10.1016/0092-8674(88)90258-9.
26. **Burley SK, Roeder RG.** 1996. Biochemistry and structural biology of transcription factor IID (TFIID). Annu Rev Biochem **65:**769–799. http://dx.doi.org/10.1146/annurev.bi.65.070196.004005.
27. **Starr DB, Hawley DK.** 1991. TFIID binds in the minor groove of the TATA box. Cell **67:**1231–1240. http://dx.doi.org/10.1016/0092-8674(91)90299-E.
28. **Bhaumik SR, Raha T, Aiello DP, Green MR.** 2004. In vivo target of a transcriptional activator revealed by fluorescence resonance energy transfer. Genes Dev **18:**333–343. http://dx.doi.org/10.1101/gad.1148404.
29. **Larschan E, Winston F.** 2001. The *S. cerevisiae* SAGA complex functions in vivo as a coactivator for transcriptional activation by Gal4. Genes Dev **15:**1946–1956. http://dx.doi.org/10.1101/gad.911501.
30. **Bhaumik SR, Green MR.** 2001. SAGA is an essential in vivo target of the yeast acidic activator Gal4p. Genes Dev **15:**1935–1945. http://dx.doi.org/10.1101/gad.911401.
31. **Dudley AM, Rougeulle C, Winston F.** 1999. The Spt components of SAGA facilitate TBP binding to a promoter at a post-activator-binding step in vivo. Genes Dev **13:**2940–2945. http://dx.doi.org/10.1101/gad.13.22.2940.
32. **Qiu H, Hu C, Zhang F, Hwang GJ, Swanson MJ, Boonchird C, Hinnebusch AG.** 2005. Interdependent recruitment of SAGA and Srb mediator by transcriptional activator Gcn4p. Mol Cell Biol **25:**3461–3474. http://dx.doi.org/10.1128/MCB.25.9.3461-3474.2005.
33. **Belotserkovskaya R, Sterner DE, Deng M, Sayre MH, Lieberman PM, Berger SL.** 2000. Inhibition of TATA-binding protein function by SAGA subunits Spt3 and Spt8 at Gcn4-activated promoters. Mol Cell Biol **20:**634–647. http://dx.doi.org/10.1128/MCB.20.2.634-647.2000.
34. **Lee CK, Shibata Y, Rao B, Strahl BD, Lieb JD.** 2004. Evidence for nucleosome depletion at active regulatory regions genome-wide. Nat Genet **36:**900–905. http://dx.doi.org/10.1038/ng1400.
35. **Lohr D, Lopez J.** 1995. GAL4/GAL80-dependent nucleosome disruption/deposition on the upstream regions of the yeast *GAL1-10* and *GAL80* genes. J Biol Chem **270:**27671–27678. http://dx.doi.org/10.1074/jbc.270.46.27671.
36. **Bryant GO, Prabhu V, Floer M, Wang X, Spagna D, Schreiber D, Ptashne M.** 2008. Activator control of nucleosome occupancy in activation and repression of transcription. PLoS Biol **6:**2928–2939. http://dx.doi.org/10.1371/journal.pbio.0060317.
37. **Lemieux K, Gaudreau L.** 2004. Targeting of Swi/Snf to the yeast *GAL1* UAS_G requires the mediator, TAF IIs, and RNA polymerase II. EMBO J **23:**4040–4050. http://dx.doi.org/10.1038/sj.emboj.7600416.
38. **Fillingham J, Recht J, Silva AC, Suter B, Emili A, Stagljar I, Krogan NJ, Allis CD, Keogh MC, Greenblatt JF.** 2008. Chaperone control of the activity and specificity of the histone H3 acetyltransferase Rtt109. Mol Cell Biol **28:**4342–4353. http://dx.doi.org/10.1128/MCB.00182-08.
39. **Chan RK, Otte CA.** 1982. Physiological characterization of Saccharomyces cerevisiae mutants supersensitive to G_1 arrest by a factor and alpha factor pheromones. Mol Cell Biol **2:**21–29. http://dx.doi.org/10.1128/MCB.2.1.21.
40. **Longtine M, McKenzie A, III, Demarini DJ, Shah NG, Wach A, Brachat A, Philippsen P, Pringle JR.** 1998. Additional modules for versatile and economical PCR-based gene deletion and modification in Saccharomyces cerevisiae. Yeast **14:**953–961.
41. **Ausubel FM, Brent R, Kingston RE, Moore DD, Seidman GG, Smith JA, Struhl K (ed).** 1987. Current protocols in molecular biology. John Wiley & Sons, New York, NY.
42. **Cavallini B, Faus I, Matthes H, Chipoulet J-M, Winsor B, Egly JM, Chambon P.** 1989. Cloning of the gene encoding the yeast protein BTF1, which can substitute for the human TATA box-binding factor. Proc Natl Acad Sci U S A **86:**9803–9807. http://dx.doi.org/10.1073/pnas.86.24.9803.
43. **Zhang L, Fletcher AG, Cheung V, Winston F, Stargell LA.** 2008. Spn1 regulates the recruitment of Spt6 and the Swi/Snf complex during transcriptional activation by RNA polymerase II. Mol Cell Biol **28:**1393–1403. http://dx.doi.org/10.1128/MCB.01733-07.
44. **Hieb AR, D'Arcy S, Kramer MA, White AE, Luger K.** 2012. Fluorescence strategies for high-throughput quantification of protein interactions. Nucleic Acids Res **40:**e33. http://dx.doi.org/10.1093/nar/gkr1045.
45. **Dechassa ML, Wyns K, Li M, Hall MA, Wang MD, Luger K.** 2011.

Structure and Scm3-mediated assembly of budding yeast centromeric nucleosomes. Nat Commun **2:**313. http://dx.doi.org/10.1038/ncomms1320.
46. **Luger K, Rechsteiner TJ, Richmond TJ.** 1999. Preparation of nucleosome core particle from recombinant histones. Methods Enzymol **304:**3–19. http://dx.doi.org/10.1016/S0076-6879(99)04003-3.
47. **Reese JC, Zhang H, Zhang Z.** 2008. Isolation of highly purified yeast nuclei for nuclease mapping of chromatin structure. Methods Mol Biol **463:**43–53. http://dx.doi.org/10.1007/978-1-59745-406-3_3.
48. **Ryan MP, Stafford GA, Yu L, Cummings KB, Morse RH.** 1999. Assays for nucleosome positioning in yeast. Methods Enzymol **304:**376–399. http://dx.doi.org/10.1016/S0076-6879(99)04023-9.
49. **Dyer PN, Edayathumangalam RS, White CL, Bao Y, Chakravarthy S, Muthurajan UM, Luger K.** 2004. Reconstitution of nucleosome core particles from recombinant histones and DNA. Methods Enzymol **375:**23–44.
50. **Park YJ, Sudhoff KB, Andrews AJ, Stargell LA, Luger K.** 2008. Histone chaperone specificity in Rtt109 activation. Nat Struct Mol Biol **15:**957–964. http://dx.doi.org/10.1038/nsmb.1480.
51. **Albert I, Mavrich TN, Tomsho LP, Qi J, Zanton SJ, Schuster SC, Pugh BF.** 2007. Translational and rotational settings of H2A.Z nucleosomes across the *Saccharomyces cerevisiae* genome. Nature **446:**572–576. http://dx.doi.org/10.1038/nature05632.
52. **Lee W, Tillo D, Bray N, Morse RH, Davis RW, Hughes TR, Nislow C.** 2007. A high-resolution atlas of nucleosome occupancy in yeast. Nat Genet **39:**1235–1244. http://dx.doi.org/10.1038/ng2117.
53. **Mavrich TN, Ioshikhes IP, Venters BJ, Jiang C, Tomsho LP, Qi J, Schuster SC, Albert I, Pugh BF.** 2008. A barrier nucleosome model for statistical positioning of nucleosomes throughout the yeast genome. Genome Res **18:**1073–1083. http://dx.doi.org/10.1101/gr.078261.108.
54. **Jiang C, Pugh BF.** 2009. A compiled and systematic reference map of nucleosome positions across the *Saccharomyces cerevisiae* genome. Genome Biol **10:**R109. http://dx.doi.org/10.1186/gb-2009-10-10-r109.
55. **Floer M, Wang X, Prabhu V, Berrozpe G, Narayan S, Spagna D, Alvarez D, Kendall J, Krasnitz A, Stepansky A, Hicks J, Bryant GO, Ptashne M.** 2010. A RSC/nucleosome complex determines chromatin architecture and facilitates activator binding. Cell **141:**407–418. http://dx.doi.org/10.1016/j.cell.2010.03.048.
56. **Johnston M, Davis RW.** 1984. Sequences that regulate the divergent *GAL1-GAL10* promoter in *Saccharomyces cerevisiae*. Mol Cell Biol **4:**1440–1448. http://dx.doi.org/10.1128/MCB.4.8.1440.
57. **West RW, Yocum RR, Ptashne M.** 1984. Yeast GAL1-GAL10 divergent promoter region: location and function of the upstream activating sequence UAS_G. Mol Cell Biol **4:**2467–2478. http://dx.doi.org/10.1128/MCB.4.11.2467.
58. **Daganzo SM, Erzberger JP, Lam WM, Skordalakes E, Zhang R, Franco AA, Brill SJ, Adams PD, Berger JM, Kaufman PD.** 2003. Structure and function of the conserved core of histone deposition protein Asf1. Curr Biol **13:**2148–2158. http://dx.doi.org/10.1016/j.cub.2003.11.027.
59. **Lowary PT, Widom J.** 1998. New DNA sequence rules for high affinity binding to histone octamer and sequence-directed nucleosome positioning. J Mol Biol **276:**19–42. http://dx.doi.org/10.1006/jmbi.1997.1494.
60. **Sharma N, Nyborg JK.** 2008. The coactivators CBP/p300 and the histone chaperone NAP1 promote transcription-independent nucleosome eviction at the HTLV-1 promoter. Proc Natl Acad Sci U S A **105:**7959–7963. http://dx.doi.org/10.1073/pnas.0800534105.
61. **Li B, Pattenden SG, Lee D, Gutierrez J, Chen J, Seidel C, Gerton J, Workman JL.** 2005. Preferential occupancy of histone variant H2AZ at inactive promoters influences local histone modifications and chromatin remodeling. Proc Natl Acad Sci U S A **102:**18385–18390. http://dx.doi.org/10.1073/pnas.0507975102.
62. **Zlatanova J, Thakar A.** 2008. H2A.Z: view from the top. Structure **16:**166–179. http://dx.doi.org/10.1016/j.str.2007.12.008.
63. **Mizuguchi G, Shen X, Landry J, Wu WH, Sen S, Wu C.** 2004. ATP-driven exchange of histone H2AZ variant catalyzed by SWR1 chromatin remodeling complex. Science **303:**343–348. http://dx.doi.org/10.1126/science.1090701.
64. **Deniz O, Flores O, Battistini F, Perez A, Soler-Lopez M, Orozco M.** 2011. Physical properties of naked DNA influence nucleosome positioning and correlate with transcription start and termination sites in yeast. BMC Genomics **12:**489. http://dx.doi.org/10.1186/1471-2164-12-489.
65. **Hornung G, Oren M, Barkai N.** 2012. Nucleosome organization affects the sensitivity of gene expression to promoter mutations. Mol Cell **46:**362–368. http://dx.doi.org/10.1016/j.molcel.2012.02.019.
66. **Bai L, Ondracka A, Cross FR.** 2011. Multiple sequence-specific factors generate the nucleosome-depleted region on CLN2 promoter. Mol Cell **42:**465–476. http://dx.doi.org/10.1016/j.molcel.2011.03.028.
67. **Jansen A, van der Zande E, Meert W, Fink GR, Verstrepen KJ.** 2012. Distal chromatin structure influences local nucleosome positions and gene expression. Nucleic Acids Res **40:**3870–3885. http://dx.doi.org/10.1093/nar/gkr1311.
68. **Jansen A, Verstrepen KJ.** 2011. Nucleosome positioning in Saccharomyces cerevisiae. Microbiol Mol Biol Rev **75:**301–320. http://dx.doi.org/10.1128/MMBR.00046-10.
69. **Perales R, Zhang L, Bentley D.** 2011. Histone occupancy in vivo at the 601 nucleosome binding element is determined by transcriptional history. Mol Cell Biol **31:**3485–3496. http://dx.doi.org/10.1128/MCB.05599-11.
70. **Vinogradov AE.** 2003. DNA helix: the importance of being GC-rich. Nucleic Acids Res **31:**1838–1844. http://dx.doi.org/10.1093/nar/gkg296.
71. **Bhaumik SR, Green MR.** 2002. Differential requirement of SAGA components for recruitment of TATA-box-binding protein to promoters in vivo. Mol Cell Biol **22:**7365–7371. http://dx.doi.org/10.1128/MCB.22.21.7365-7371.2002.
72. **Byrum S, Mackintosh SG, Edmondson RD, Cheung WL, Taverna SD, Tackett AJ.** 2011. Analysis of histone exchange during chromatin purification. J Integr OMICS **1:**61–65.
73. **Byrum SD, Taverna SD, Tackett AJ.** 2011. Quantitative analysis of histone exchange for transcriptionally active chromatin. J Clin Bioinform **1:**17. http://dx.doi.org/10.1186/2043-9113-1-17.
74. **Radman-Livaja M, Verzijlbergen KF, Weiner A, van Welsem T, Friedman N, Rando OJ, van Leeuwen F.** 2011. Patterns and mechanisms of ancestral histone protein inheritance in budding yeast. PLoS Biol **9:**e1001075. http://dx.doi.org/10.1371/journal.pbio.1001075.
75. **Das C, Tyler JK.** 2013. Histone exchange and histone modifications during transcription and aging. Biochim Biophys Acta **1819:**332–342.
76. **Rowe CE, Narlikar GJ.** 2010. The ATP-dependent remodeler RSC transfers histone dimers and octamers through the rapid formation of an unstable encounter intermediate. Biochemistry **49:**9882–9890. http://dx.doi.org/10.1021/bi101491u.
77. **Xue YM, Kowalska AK, Grabowska K, Przybyt K, Cichewicz MA, Del Rosario BC, Pemberton LF.** 2013. Histone chaperones Nap1 and Vps75 regulate histone acetylation during transcription elongation. Mol Cell Biol **33:**1645–1656. http://dx.doi.org/10.1128/MCB.01121-12.
78. **Del Rosario BC, Pemberton LF.** 2008. Nap1 links transcription elongation, chromatin assembly, and messenger RNP complex biogenesis. Mol Cell Biol **28:**2113–2124. http://dx.doi.org/10.1128/MCB.02136-07.
79. **Walfridsson J, Khorosjutina O, Matikainen P, Gustafsson CM, Ekwall K.** 2007. A genome-wide role for CHD remodelling factors and Nap1 in nucleosome disassembly. EMBO J **26:**2868–2879. http://dx.doi.org/10.1038/sj.emboj.7601728.